Astron. Astrophys. 287, 824–828 (1994)

ASTRONOMY AND ASTROPHYSICS

Localizations and spectra of gamma-ray bursts observed within the sidelobes of the SIGMA telescope

A. Claret[1], F. Lebrun[1], J. Paul[1], B. Cordier[1], F. Pelaez[2], E. Jourdain[2], M. Niel[2], J.-P. Roques[2], O. Terekov[3], V. Lobachev[3], D. Denisenko[3], R. Sunyaev[3], E. Churazov[3], M. Gilfanov[3], A. Dyachkov[3], and N. Khavenson[3]

[1] Service d'Astrophysique, Centre d'Etudes Nucléaires de Saclay, F-91191 Gif-sur-Yvette Cedex, France
[2] Centre d'Etude Spatiale des Rayonnements, 9 Av du Colonel Roche, BP 4346, F-31029 Toulouse Cedex, France
[3] Space Research Institute, Profsouznaya, 84/32, 117296 Moscow, Russia

Received 13 December, 1993; Accepted 28 December, 1993

Abstract. Two cylindrical interruptions of the SIGMA telescope passive shield act as collimators, projecting arc-shaped images on the detector. The field of view (FOV) of these collimators consists of significant sidelobes in the SIGMA sensitivity diagram. GRB localizations, provided by this imaging system, can be combined with the annulus derived from triangulation with other spacecraft, in order to provide a narrow window for the search for counterparts at other wavelengths. 4 cosmic gamma-ray bursts (GRBs) have been detected so far by the lower collimator. Localizations with an accuracy of a fraction of degree, as well as time structures and broad band spectroscopy in the 30-400 keV energy range, of these 4 GRBs are presented.

Key words: gamma rays: bursts – observational methods

1. Introduction

The SIGMA experiment on board *GRANAT* (Paul et al. 1991) offers the possibility of locating GRBs, within the 17.9° by 16.7° FOV of the coded mask, with a few arc min. accuracy. In spite of the high sensitivity of the telescope in its burst mode (3.4 10^{-7} and 1.2 10^{-7} erg s^{-1} cm^{-2} in the 30-1000 keV band) (Pelaez 1993a), no burst was detected so far within the coded FOV (Sunyaev et al. 1993).

Any bright γ-ray source, located less than 35° away from the pointing axis of SIGMA, projects an arc-shaped image on the detector through one of the two interruptions in the cylindrical passive shield of the telescope. These interruptions act as collimators whose FOV consists of sidelobes in the SIGMA sensitivity diagram. The upper collimator enables the acquirement of high angular resolution images in the 35-200 keV band. The lower one offers a much higher sensitive area up to 300 keV to the detriment of angular resolution. The reader is referred to Claret et al. (1994a) for a complete description of this imaging system and its in-flight performance. Thanks to the significant FOV, the sidelobes of SIGMA are well suited for the localization of GRBs. 4 cosmic GRBs (see Table 1) have been detected and localized by the lower collimator (Claret et al. 1994b). The cosmic origin of these 4 GRBs has been confirmed by the experiments of the 3[rd] Interplanetary Network (*CGRO*, *ULYSSES* and *PVO*), and also by PHEBUS on board *GRANAT* (private communication from C. Barat and J.-P. Dezalay).

In this paper, we present a short review of the GRB fast routine localization system of SIGMA for the search for counterparts at other wavelengths (Sect. 2). Localizations, as well as

Table 1. Summary of GRBs localized within the sidelobes

	GRB910122	GRB920714
Trigger time (UT)	$15^h13^{mn}48.564^s$	$13^h04^{mn}31.014^s$
Event duration	≈ 120 s [c]	28.7 s
Record in burst mode	42.6 s	50.8 s
Flux[a,b] at 100 keV	4.14 ± 0.13	1.94 ± 0.10
Power Law Index[a]	-1.75 ± 0.05	-1.68 ± 0.10
Reduced χ^2 (dof)	1.14 (6)	0.76 (6)
	GRB920723	**GRB930310**
Trigger time (UT)	$20^h03^{mn}08.323^s$	$07^h20^{mn}07.290^s$
Event duration	6.2 s	10.7 s
Record in burst mode	14.5 s	53 s
Flux[a,b] at 100 keV	20.46 ± 0.60	1.71 ± 0.10
Power Law Index[a]	-1.00 ± 0.05	-1.71 ± 0.11
Reduced χ^2 (dof)	2.63 (6)	0.78 (6)

[a] 68% confidence level in a single parameter
[b] 10^{-2} ph cm^{-2} s^{-1} keV^{-1} unit
[c] Total duration recorded in the slow variability mode

Send offprint requests to: A. Claret

light curves and broad band spectroscopy, of GRBs observed within the sidelobes are reported in Sect. 3.

2. SIGMA contribution for localizing GRBs

The GRB detection system of the SIGMA telescope is decribed in Guerry et al. (1986). The in-flight check of the location accuracy, achievable for GRBs observed through the coded mask, has been addressed in Sunyaev et al. (1993). Only the opportunity of imaging GRBs within the sidelobes is discussed here.

The sidelobes significantly enlarge the FOV of SIGMA. They offer two detection cells of $\approx$ 500 and $\approx$ 2700 square degrees, surrounding the $\approx$ 125 square degrees of the coded mask cell (at half sensitivity). The imaging process within sidelobes is based on the analysis of the arc position and orientation, using the maximum likelihood method. Bright sources can be localized by the upper and the lower collimator with a respective accuracy of 6 and 25 arc min. along the great circle connecting the pointing direction to the source direction, 26 and 130 arc min. along the perpendicular direction (Claret et al. 1993). For comparison, the all sky monitor WATCH, on board *GRANAT*, provides burst location error boxes of 1° radius. The typical error box of BATSE/*CGRO* is 4-10° radius in the burst mode (Meegan et al. 1992). Some GRBs detected by BATSE are potential candidates for imaging since they are in the FOV of COMPTEL/*CGRO*. The maximum likelihood method, applied to selected events recorded by COMPTEL in telescope mode, led to localizations of 4 GRBs to within 1-5° (Connors et al. 1993).

Localizations with an accuracy of a fraction of degree, as well as light curves and broad band spectroscopy, of GRBs observed with this imaging system are of interest to the astronomical community. Multiwavelength searches for counterparts to GRB sources require an accurate (arc min. level) localization of the event. In the γ-ray domain, such an accuracy is achievable only by the use of either the coded-mask technique or the triangulation method (see Hurley et al. 1993a and Hurley et al. 1993b about results of the 3rd Interplanetary Network). The position recovery of a burst event observed within the SIGMA sidelobes offers an independent method of localization. It permits to check the error box derived by triangulation. Moreover, when the burst arrival time method yields only one annulus (e.g. when only two spacecraft of the network have detected the event), the SIGMA error box provides a significant restriction along this annulus. Then, the resulting error box becomes small enough to encourage rapid follow-up observations at other wavelengths.

No quiescent counterparts at any wavelength were found within the arcminute error boxes derived from timing comparisons among widely separated spacecraft (Schaefer 1992), except for the well-known GRB790305 (Cline et al. 1980). Another exception is the repeater SGR 1806-20, which has been tentatively identified with SNR G10.0-0.3 in the soft X-ray and radio bands (Kulkarni et al. 1993a and 1993b, Tanaka et al. 1993). This highlights the need to search for variable (not only quiescent) counterparts to GRB sources, and subsequently to strongly reduce the processing time of burst locations. Work was done towards the goal of reducing the localization delay to within one hour after the whole content of the SIGMA memory has been downlinked to the ground station. Prompt localizations are thus derived at the ground station, using a simple algorithm (the fast routine localization) instead of the maximum likelihood method. The most important remaining delay (about a few days), between the GRB detection and the communication of its error box, is related to the publication of an IAU circular after the agreement of all laboratories involved in the SIGMA experiment.

3. Observations and data analysis

3.1. Localizations

The position recovery process of a source observed through the sidelobes is described in Claret et al. (1993). It consists in analysing the arc position and orientation in the detector image. For each bin (α, δ) of the sky, the modelled response of the collimator is compared to the data counts in each pixel of the image, using the standard maximum-likelihood method appropriate for Poisson statistics. Both the source flux and background level are allowed to vary. Contours of constant probability are mapped in the (α, δ) space, at the equivalent of $1, 2$ and $3\,\sigma$ significance for the case of two parameters (Fig. 1.). The resulting error boxes are crescent-shaped due to the nearly circular symmetry of the arc images. The location accuracy is better than half a degree for the brightest bursts. SIGMA localizations are fully compatible with those obtained by triangulation using timing information from the 3rd Interplanetary Network.

Prompt localizations of the three latest events were processed at the ground station, using the fast routine localisations algorithm. This algorithm does not take into account neither the complex shape of the arc images, nor the energy response of the collimating system. For each bin (α, δ) of the sky, a measure of the signal-to-noise ratio is derived by considering the recorded counts within the predicted arc area. The corresponding error boxes were then reported in IAU circulars (Claret et al. 1992 and Goldwurm et al. 1993). It appears that the $2\,\sigma$ error boxes derived from the fast routine localisation are in good agreement with those derived from the likelihood method (Fig. 1.).

3.2. Timing and spectral analysis

The onboard SIGMA memory, allocated for the burst recording, is limited. Once the position coordinates and the energy deposit of 32256 photons (28224 after the trigger event, 4032 before) have been stored, the telescope returns to its nominal imaging mode, till an eventual second trigger. In the case of GRB910122, the camera burst data consist of a $\approx$ 43 s record, while the total duration of the event is $\approx$ 120 s as recorded by the slow variability mode (Paul et al. 1991). For the three other bursts, the complete time histories were recorded in the burst mode of the telescope (see Table 1). In order to search for spectral evolution during the bursts, hardness ratios have been derived considering energy integrated and background-subtracted count-rates. Only

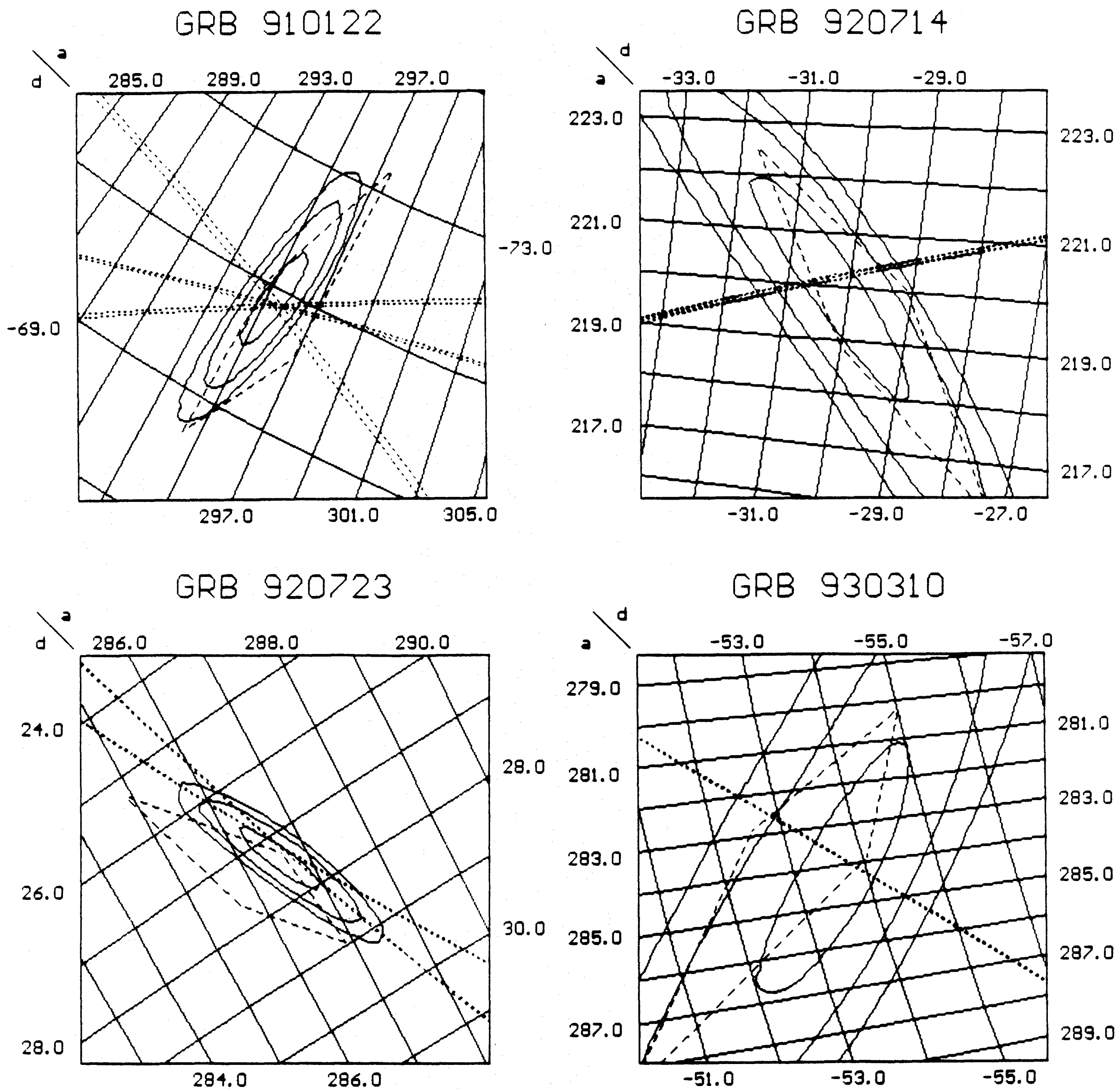

Fig. 1. GRB localizations obtained by SIGMA in the 30-200 keV range: contours correspond to 1σ, 2σ and 3σ confidence intervals. The positions obtained by triangulation with the spacecraft of the 3rd Interplanetary Network are also shown (personal communication from K. Hurley). The 2 σ error boxes derived by the fast routine localization (see text) are represented by dashed diamonds

the two brightest events (GRB910122 and GRB920723) show a significant hard-to-soft spectral evolution (Fig. 2.).

Time-integrated, deadtime corrected and background subtracted energy spectra have been derived for each burst (Fig. 3.). Thanks to the imaging capability of the collimating system, the background can be measured during the burst, rather than being estimated prior to the burst detection. Observations of the Crab nebula within the SIGMA sidelobes have been used in order to assess the energy response of the collimators. Results of fits with a single power law model in the 35-400 keV range are given in Table 1. For GRB920723, a better fit is obtained by considering a sum of two power laws, with one of the two photon indexes fixed at -1.7 (the average index of the other bursts). The fluxes at 100 keV of each contribution are 9.94 ± 0.49 and 9.19 ± 0.43 10^{-2} ph cm^{-2} s^{-1} keV^{-1} respectively. The photon index of the second contribution is -0.42 $\pm$ 0.2. The reduced χ^2 becomes then 1.3 (dof = 5).

The two bursts which occured in July 1992 (GRB920714 and GRB920723) were also detected by the anticoïncidence shield of SIGMA. The corresponding spectra are well fitted with power law models (Pelaez et al. 1993b) slightly softer than those recorded by the gamma-camera. These small discrepancies could result from the differences in energy ranges and/or time intervals which were considered in the fitting procedures. Moreover, the spectrum of these bursts is not necessarily well described by a single power law over the whole energy range covered by the two SIGMA GRB detectors (30-400 keV for the gamma-camera and 0.7-15 MeV for the anticoïncidence shield).

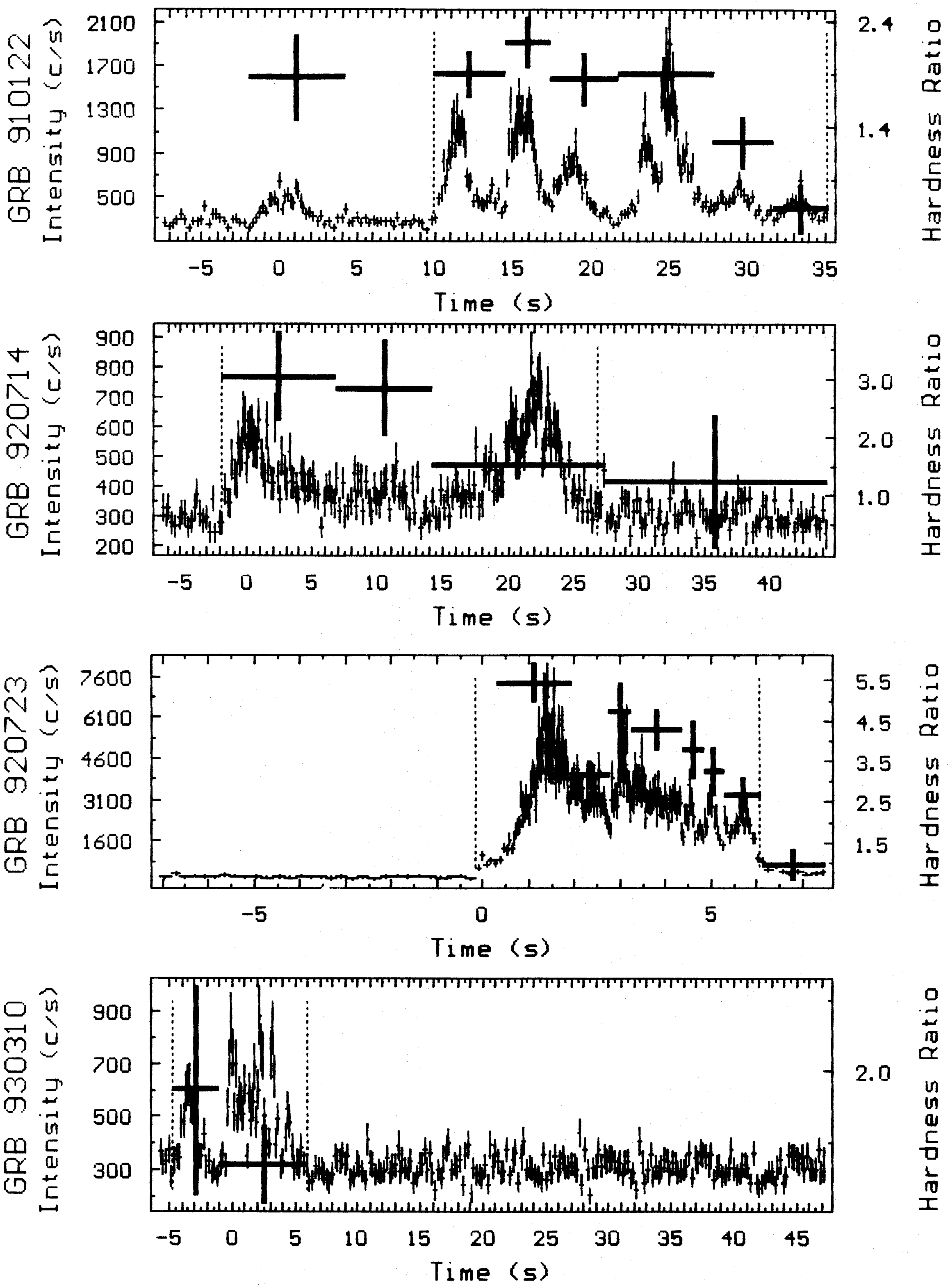

Fig. 2. The ratio of counts in the 150-300 keV band to that in the 40-75 keV band is plotted (thick crosses, right axis) together with the total count-rate in the 30-200 keV energy range (thin crosses, left axis). The dotted lines indicate the time interval used to derive the spectrum of each burst (see Table 1)

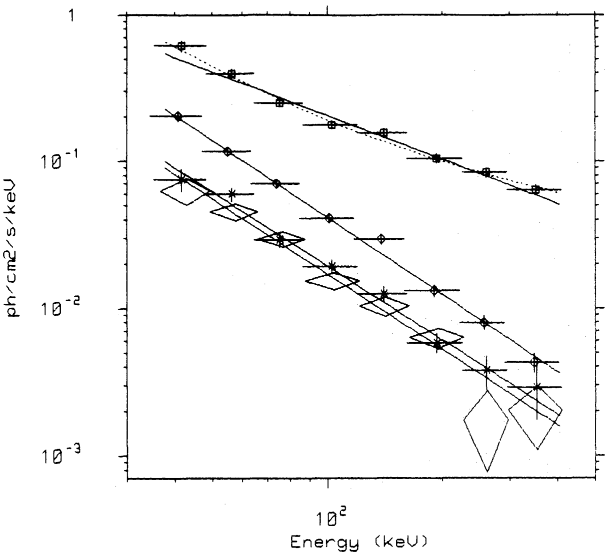

Fig. 3. The average photon spectra of GRB910122 (circles), GRB920714 (stars), GRB920723 (squares) and GRB930310 (diamonds) are represented together with their single power law best fit. For GRB920723, the best fit for a sum of two power laws is also indicated (dotted line)

Finally, there may be also a small but systematic hardening of spectra recorded by the gamma-camera, due to the pile up of several electronic pulses at very high count-rate (up to 10^4 count/s for GRB920723).

4. Conclusion

Among the experiments capable to give a localization of GRBs based only upon their own data (BATSE, COMPTEL, WATCH ...), SIGMA provides the best location accuracy. The 4 GRBs observed within the sidelobes of the SIGMA telescope have been located with an accuracy of a fraction of degree. All localizations derived so far are fully compatible with those obtained by independent methods using triangulation with other spacecraft. The spectral analysis of these 4 GRBs leads to photon spectra which can be described by single power laws (GRB910122, GRB920714 and GRB930310) or a sum of two power laws (GRB920723).

Acknowledgements. The 3rd Interplanetary Network (*CGRO*, *ULYSSES* and *PVO*) error boxes are courtesy of K. Hurley, M. Sommer, J. Fishman, C. Meegan, C. Kouveliotou, J. Laros and R. Klebesadel.

References

Claret, A., Jourdain, E., Churazov, E., et al., 1992, *IAU Circ. 5579*
Claret, A., Lebrun, F., Laurent, L., et al., 1994a, A&A, in press
Claret, A., Lebrun, F., Laurent, L., et al., 1994b, in: Gehrels N., Dennis B. (eds.) Proc. 2nd Compton Observatory Science Workshop, 1993 Sept. 20-22, College Park, in press
Cline, T. et al., 1980, ApJ 255, L45
Connors, A., Aarts, H.J.M., Bennett, K., et al., 1993, A&AS 97, 75
Goldwurm, A., Schmitz-Fraysse, M.-C., Churazov, E., et al., 1993, *IAU Circ. 5720*
Guerry, A., Jouret, M., Roques, J.-P., et al., 1986, Adv. Space Res. 6, No. 4, 103
Hurley, K., Sommer, M., Cline, T., et al., 1993a, in: Proc. of the Arthur Holly Compton Centennial Symposium on Gamma-Ray Astronomy, Results from the Gamma-Ray Observatory, AIP Conf. Proc 280, St Louis, p.769
Hurley, K., Sommer, M., Boer, M., et al., 1993b, A&AS 97, 39
Kulkarni, S., Frail, D., Kassim, N., et al., 1993a, *IAU Circ. 5879*
Kulkarni, S., Matthews, K., Neugebauer, G., et al., 1993b, *IAU Circ. 5883*
Meegan, C.A., Fishman, G.J., Wilson, R.B., et al., 1992, Nature, 355, 143
Paul J., Mandrou P., Ballet J., et al., 1991, Adv. Space Res. 11, No. 8, 289
Pelaez, F., 1993a, Thèse de Doctorat de l'Université Paul Sabatier (Toulouse), N° 1483
Pelaez, F., Bouchet, L., Jourdain, E., et al., 1993b, ApJS, in press
Schaefer, B. E., 1992,in: Ho C., Epstein R.I., Fenimore E.E. (eds.) Proc. of the Los Alamos Workshop on Gamma-Ray Bursts, 107
Sunyaev, R., Churazov, E., Gilfanov, M., et al., 1993, ApJ 402, 579
Tanaka, Y. 1993, *IAU Circ. 5880*

This article was processed by the author using Springer-Verlag LaTeX A&A style file version 3.